



SHORT-ROOT paralogs mediate feedforward regulation of D-type cyclin to promote nodule formation in soybean

Chunhua Wang^{a,b,1}, Meng Li^{a,b,1}, Yang Zhao^{a,b,1}, Nengsong Liang^{a,b}, Haiyang Li^{a,b}, Pengxue Li^{a,b}, Liling Yang^{a,b}, Mengyuan Xu^{a,b}, Xinxin Bian^{a,b}, Mengxue Wang^{a,b}, Shasha Wu^{a,b}, Xufang Niu^{a,b}, Mengyao Wang^{a,b}, Xinxin Li^{a,b}, Yi Sang^c, Wentao Dong^d, Ertao Wang^d, Kimberly L. Gallagher^e, and Shuang Wu^{a,b,2}

^aCollege of Horticulture, Fujian Agriculture and Forestry University, Fuzhou 350002, China; ^bCollege of Life Sciences, Fujian Agriculture and Forestry University, Fuzhou 350002, China; ^cSchool of Life Sciences, Lanzhou University, Lanzhou 730000, China; ^dShanghai Institutes for Biological Sciences, Chinese Academy of Sciences, Shanghai 200032, China; and ^eDepartment of Biology, University of Pennsylvania, Philadelphia, PA 19104

Edited by Natasha Raikhel, Department for Botany and Plant Science, University of California, Center for Plant Cell Biology, Riverside, CA; received May 8, 2021; accepted November 5, 2021

Nitrogen fixation in soybean takes place in root nodules that arise from de novo cell divisions in the root cortex. Although several early nodulin genes have been identified, the mechanism behind the stimulation of cortical cell division during nodulation has not been fully resolved. Here we provide evidence that two paralogs of soybean SHORT-ROOT (GmSHR) play vital roles in soybean nodulation. Expression of GmSHR4 and GmSHR5 (GmSHR4/5) is induced in cortical cells at the beginning of nodulation, when the first cell divisions occur. The expression level of GmSHR4/5 is positively associated with cortical cell division and nodulation. Knockdown of GmSHR5 inhibits cell division in outer cortical layers during nodulation. Knockdown of both paralogs disrupts the cell division throughout the cortex, resulting in poorly organized nodule primordia with delayed vascular tissue formation. GmSHR4/5 function by enhancing cytokinin signaling and activating early nodulin genes. Interestingly, D-type cyclins act downstream of GmSHR4/5, and GmSHR4/5 form a feedforward loop regulating D-type cyclins. Overexpression of D-type cyclins in soybean roots also enhanced nodulation. Collectively, we conclude that the GmSHR4/5-mediated pathway represents a vital module that triggers cytokinin signaling and activates D-type cyclins during nodulation in soybean.

nodule primordia | GmSHR4/5 | cell division | cytokinin | GmCYCD6;1

Nodulation in legumes is coordinated by two coordinated processes: rhizobial infection and nodule formation (1, 2). Studies over the past decade have identified key components of the Nod factor-activated signaling pathway in the early symbiotic stage (3–6). Nodule organogenesis starts with new cell divisions in root cortical tissues (4). The root cortex in soybean consists of multiple layers, and the Nod factor-induced cell division occurs first in the outer cortical cells followed by divisions in the inner cortical tissues and the pericycle (7). A number of regulators of Nod factor perception have been identified, including NODULE INCEPTION (NIN) (8), an ERF family protein (ERN), and two GRAS family proteins called Nodulation Signaling Pathway (NSP1 and NSP2) (4–6). Overexpression of *NIN* in the absence of rhizobia is sufficient to induce cortical cell divisions and leads to spontaneous nodule-like structures (9). *ENOD40*, a marker gene for nodule primordium initiation, is up-regulated at the onset of nodulation (10–12). These Nod factor-inducible genes can be directly activated by NSP1 (13). The soybean orthologs of all these components have been identified (14).

In addition to the transcriptional regulators, the phytohormone cytokinin (CK) also plays a key role in promoting cortical cell division in the early symbiotic stages (15–25). Depletion of the endogenous CK by overexpressing a CK oxidase/dehydrogenase (CKX)

or by repressing expression of the cytokinin biosynthetic gene *LONELY GUY 1 (LOG1)* dramatically decreases nodulation in *Lotus japonicus* and *Medicago truncatula* (25, 26). The crucial role of cytokinin is also evidenced by the effects of overexpressing *ARABIDOPSIS THALIANA RESPONSE REGULATOR 5 (ARR5)*, *MtRR4 type-ARR*, or *Two-Component Signaling Sensor (TCS)*, all of which increase cortical cell divisions and nodulation (19, 27). Interestingly, gain-of-function mutants of both *LOTUS HISTIDINE KINASE 1 (LHK1)* (*L. japonicus lotus*, named *snf2*) and Cytokinin Response 1 (*MtCRE1*) result in “spontaneous nodule formation” in the absence of rhizobia (24). Genetic analyses indicate that the spontaneous nodule formation in *snf2* requires *NIN* and *NSP2* (24).

As nodules form on roots, it has been hypothesized that nodule organogenesis is derived from the lateral root developmental program (5, 28–31). Recent studies in *M. truncatula* showed that several transcription factors, including WUS-RELATED HOMEBOX 5 (*MtWOX5*) and *MtPLETHORA*, are expressed

Significance

Nitrogen fixation is economically important in agriculture. Enhancing nodulation in soybean can greatly enhance nitrogen fixation efficiency. Nodule formation in legumes starts with cortical cell divisions in the root. Despite the discovery of the Nod factors and plant hormones that are involved, it remains unclear how cortical cell division is spatiotemporally regulated. Here we provide evidence that soybean has acquired two SHORT-ROOT (SHR) paralogs during evolution, which are specifically induced in the early stage of nodule organogenesis. These SHR homologs can activate the expression of early nodulin genes and enhance cytokinin signaling and form part of a multilevel regulatory network to activate D-type cyclins during nodulation. Our results provide insight into the mechanisms of nodule organogenesis in soybean.

Author contributions: C.W. and Shuang Wu designed research; C.W., M.L., Y.Z., N.L., H.L., P.L., L.Y., M.X., X.B., Mengxue Wang, Shasha Wu, X.N., and Mengyao Wang performed research; X.L. contributed new reagents/analytic tools; C.W. analyzed data; and C.W., Y.S., W.D., E.W., K.L.G., and Shuang Wu wrote the paper.

The authors declare no competing interest.

This article is a PNAS Direct Submission.

This open access article is distributed under Creative Commons Attribution-NonCommercial-NoDerivatives License 4.0 (CC BY-NC-ND).

¹C.W., M.L., and Y.Z. contributed equally to this work.

²To whom correspondence may be addressed. Email: wus@fafu.edu.cn.

This article contains supporting information online at <http://www.pnas.org/lookup/suppl/doi:10.1073/pnas.2108641119/-DCSupplemental>.

Published January 12, 2022.

and function in the nodule meristem (32–34). In addition, RNA-seq of laser-microdissected nodules showed that close homologs for a series of key root meristem regulators are expressed in nodule primordia, including *WOX5*, *ARABIDOPSIS CRINKLY 4* (*ACR4*), *SHORT-ROOT* (*SHR*), *PLT*, *SCARECROW* (*SCR*), and *JACKDAW* (*JKD*) (34). In *Arabidopsis* roots, *SHR* and *SCR* activate the expression of a D-type cyclin, *CYCD6;1* to promote the periclinal division, which separates endodermis and cortex cell layers (35). Recently, it was revealed that *MtSHR* and *MtSCR* from *M. truncatula* form the module to drive the cell division in the cortex during nodule formation (36). These findings provided a hint that root developmental programs might be involved in nodulation. However, the function of important root meristem genes in nodule organogenesis has not been fully explored.

In this study, we obtained evidence that two distally evolved paralogs of the GRAS family protein *SHR* (*GmSHR4* and *GmSHR5*) regulate cortical cell divisions and nodule organogenesis in soybean. After inoculation with rhizobia, *GmSHR4/5* were activated mostly in outer cortical cells where the first cell divisions occur. Overexpression of *GmSHR4/5* resulted in a substantial increase in nodulation, whereas *GmSHR4/5-microRNA* roots formed significantly fewer nodules. The expression of *GmSHR4/5* in the cortex enhanced cytokinin signaling and up-regulated the early nodulin genes. Downstream of this cascade were a set of D-type cyclins, which were regulated by a classic feedforward mechanism mediated by *GmSHR* paralogs. Therefore, our results revealed a mechanism regulating nodule primordia formation in soybean.

Results

GmSHR Paralogs Are Induced in Cortical Tissues at the Early Stage of Nodulation. In *Glycine max*, we identified six *SHR* homologs (named *GmSHR1* to *GmSHR6*) by BLAST searches using *AtSHR* protein sequences as the query. The amino acid sequence of all six homologs had the five conserved domains of typical GRAS proteins, including *LHR1*, *VHIIID*, *LHRII*, *PFYRE*, and *SAW* (*SI Appendix, Fig. S1*). Phylogenetic analysis revealed that *GmSHR1*, *GmSHR2*, *GmSHR3*, and *GmSHR6* are closely related to *Arabidopsis SHR* (*AtSHR*) and *Medicago SHR*s (*Medtr5g015490.1* and *Medtr4g097080*) (*SI Appendix, Fig. S2A*). Interestingly, two paralogs that arose during evolution of the soybean genome—*GmSHR4* and *GmSHR5*—are only distally related to *AtSHR* (*SI Appendix, Fig. S2A*). These two *GmSHR* paralogs exhibited a tissue-specific expression pattern distinct from those of the other soybean *SHR*s (*SI Appendix, Fig. S2B*). In addition, the expression of *GmSHR4* and *GmSHR5* (*GmSHR4/5* hereafter) in the roots was dramatically enhanced at 1 d after inoculation (dai) with rhizobia and then decreased with the progression of root nodulation (*SI Appendix, Fig. S2C*). By contrast, *GmSHR1* did not appear to be up-regulated until 7 dai and its expression peaked in the mature nodule at 28 dai. Expression of *GmSHR2* showed enhancement only in the mature nodule, while that of *GmSHR3* and *GmSHR6* changed very little during nodulation (*SI Appendix, Fig. S2C*). These results suggest that *GmSHR*s might participate in different stages of nodulation and *GmSHR4/5* could be involved in the initiation stage.

Within the 2-kb promoter regions upstream of *GmSHR4/5*, we identified many nodulin consensus sequence motifs (*NODCON1GM* and *NODCON2GM*) (*SI Appendix, Fig. S2D*). This implies that *GmSHR4/5* expression could be triggered by the rhizobial infection. To understand the spatiotemporal expression pattern of *GmSHR4/5* during nodulation, we first examined the nodule organogenesis in soybean roots. We performed histological visualization and divided the early nodule development into six stages (I to VI). We numbered the cortical layers from the outermost to the innermost (C1 to C5). In stages I and II, anticlinal divisions were initiated in the C1 layer and then

occurred in C2 (*SI Appendix, Fig. S3 A, B, G and H*). In stage III, inner cortical cells started to divide (in C3 to C5), and more anticlinal divisions occurred in the C1 and C2 layers (*SI Appendix, Fig. S3 C and J*). In stage IV, divisions occurred in the endodermis and periclinal divisions started in the C1 layer (*SI Appendix, Fig. S3 D and J*). The pattern of cell divisions in the C1 layer also became more complex, leading to the formation of a primordial structure (*SI Appendix, Fig. S3 D and J*). In stage V, most of the cortical cells at the infection site had divided into smaller cells and cells in the pericycle started to divide (*SI Appendix, Fig. S3 E and K*). At stage VI, the young nodules distended (*SI Appendix, Fig. S3 F and L*). The newly formed nodules underwent steady growth and differentiation, in particular forming vascular bundles in stages VII through IX (*SI Appendix, Fig. S3 M–O*). To verify these histological observations, we performed in situ hybridization of the cell-cycle marker gene *GmCyclB1.1*. In stage V, the staining first became enriched mostly in the outer cortical cells (*SI Appendix, Fig. S3P*), followed by a high level of staining in the inner cortical cells, indicating a gradual expansion of mitotic activity during early nodulation (*SI Appendix, Fig. S3Q*). Consistent with the *GmSHR4/5* expression pattern, *GmCyclB1.1* expression gradually became undetectable in mature nodules (*SI Appendix, Fig. S3 R and S*). Further, we constructed promoter:GUS reporters of *GmSHR4* and *GmSHR5*. In soybean roots, *GmSHR4* had a weak expression and could occasionally be detected in the endodermal cells, vascular tissues, and cortex cells in the mature zone (Fig. 1A). *GmSHR5* was expressed in the meristem (Fig. 1I) and confined only in vascular tissues in the mature zone (Fig. 1J and K). Upon inoculation with rhizobia, the expression of *GmSHR4/5* was greatly enhanced (Fig. 1B, L, and M). *GmSHR4/5* expression was enriched in the outer cortical tissues during the early stage of nodulation (stages II to VI) (Fig. 1C–E, M, and N) and also maintained a weak expression in the inner cortex (Fig. 1D, E, M, and N). *GmSHR4/5* expression gradually disappeared as the nodules matured (Fig. 1F–H and O–Q).

The spatiotemporal expression pattern of *GmSHR4/5* shown by the promoter GUS reporters was validated by in situ hybridization (Fig. 1R–Y), further suggesting the potential involvement of these two *SHR* paralogs in the early stage of the nodulation. Unlike *GmSHR4/5*, *GmSHR1/2* were expressed only in the vascular tissues (*SI Appendix, Fig. S2E*).

GmSHR4/5 Promote Cortical Cell Division and Positively Regulate Root Nodulation. To examine *GmSHR4/5* function, we manipulated their expression by overexpression (*OX-GmSHR4/5* hereafter) and knockdown (*GmSHR4-amiR*, *GmSHR5-amiR*, and *GmSHR4/5-amiR* hereafter) in soybean roots (Fig. 2A and *SI Appendix, Fig. S4 A–D*). Interestingly, the expression of other *GmSHR*s appeared to be moderately reduced in the *OX-GmSHR4/5* lines and increased in the *GmSHR4/5-amiR* roots, suggesting the existence of potential feedback inhibition among *GmSHR*s (*SI Appendix, Fig. S4A*).

In *Arabidopsis*, *SHR* regulates periclinal cell division in cortical initial cells (35, 37). Therefore, we examined the cortical cell layers that are derived from periclinal cell divisions in soybean roots. As expected, the *OX-GmSHR4/OX-GmSHR5* roots showed three to six additional layers of cortical tissues, while the *GmSHR4/5-amiR* roots had fewer (Fig. 2B–F). In addition, we transformed *Arabidopsis* with *GmSHR4* and *GmSHR5* and observed extra cell divisions in the cortical tissues of the transgenic plants (Fig. 2G–I). These results suggest that *GmSHR4/5* can induce cortical cell divisions.

Next, we evaluated the nodulation of soybean roots with altered *GmSHR4/5* expression at 28 dai with rhizobia. The total number and dry weight of nodules were significantly higher on *OX-GmSHR4/5* roots and substantially lower on *GmSHR4/5-amiR* roots (Fig. 2J and K and *SI Appendix, Fig. S4E*), indicating that *GmSHR4/5* functioned as the positive regulators of soybean

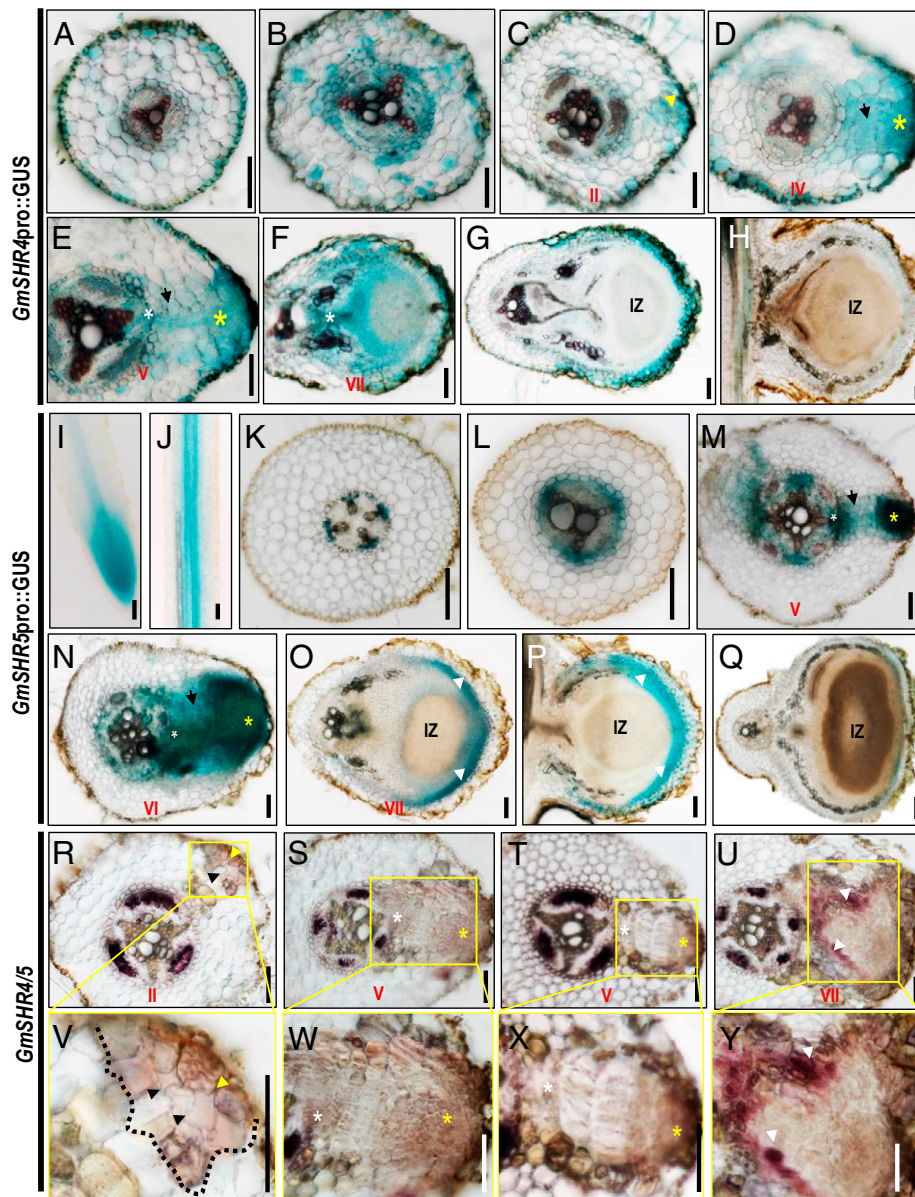


Fig. 1. Spatial expression pattern of *GmSHR* genes during nodulation in soybean. (A–H) *GmSHR4pro::GUS* expression pattern during nodulation. The cross-sections of the roots without rhizobial infection (A) and the roots at 10 dai with rhizobia (B–G) and 20 dai (H) are shown. (I–Q) *GmSHR5pro::GUS* expression pattern during nodulation. The cross-sections of the roots at 0 dai (I–K), 10 dai (L–P), and 20 dai (Q) are shown. (R–U) In situ hybridization of *GmSHR4/5* in roots at 10 dai. (V–Y) The areas in the yellow wireframe are the enlarged views of the boxed regions in R–U. IZ, infection zone. White arrows indicate the nodule parenchyma. Yellow and black arrows indicate the division of the outer cortical cells and inner cortical cells, respectively. White asterisks point to the division of the pericycle cells. Yellow asterisks point to the outer ground tissues. (Scale bars, 100 μ m.)

nodulation. Interestingly, unlike *GmSHR5-amiR*, *GmSHR4-amiR* did not change the nodulation (Fig. 2L). This finding suggests that *GmSHR5* could be more involved than *GmSHR4* in the initiation of nodule primordia.

To rule out the potential artifacts that can arise from overexpression, we specifically expressed *GmSHR4/5* in nodule primordia under the promoter of *GmENOD40*. Both *pENOD40-GmSHR4* and *pENOD40-GmSHR5* lines resulted in a higher number of nodules (Fig. 2M–P). The total dry weight of nodules of the *pENOD40-GmSHR4* and *pENOD40-GmSHR5* lines was 2.72 and 2.19 times that of the control, respectively (Fig. 2Q). These data further support that *GmSHR4/5* function in nodule formation.

***GmSHR4/5* Function in Cortical Tissues during the Nodule Initiation.**

The spatial expression pattern of *GmSHR4/5* in the cortical

tissues suggests they could be involved in the division of cortical tissues. We next examined the effect of silencing *GmSHR4/5* on the cortical cell division pattern. In *GmSHR4-amiR* roots, we detected no noticeable change in the nodulation process, suggesting the existence of functional redundancy (Fig. 3A and *SI Appendix*, Fig. S3F and L). In *GmSHR5-amiR* roots, however, we observed fewer cell divisions in the outer cortical layers, along with a disordered pattern of division (Fig. 3B and C and *SI Appendix*, Fig. S3J and K). The simultaneous silencing of *GmSHR4/5* disrupted the division pattern throughout the cortex (Fig. 3D–I and *SI Appendix*, Fig. S3J–L) and delayed the formation of the vascular tissues in the nodule primordia (Fig. 3J–L and *SI Appendix*, Fig. S3M–O). These results suggest that *GmSHR5* is more important for the initial cell divisions in outer cortical layers, but both *GmSHR4* and -5 redundantly promote ordered cortical cell divisions to form a

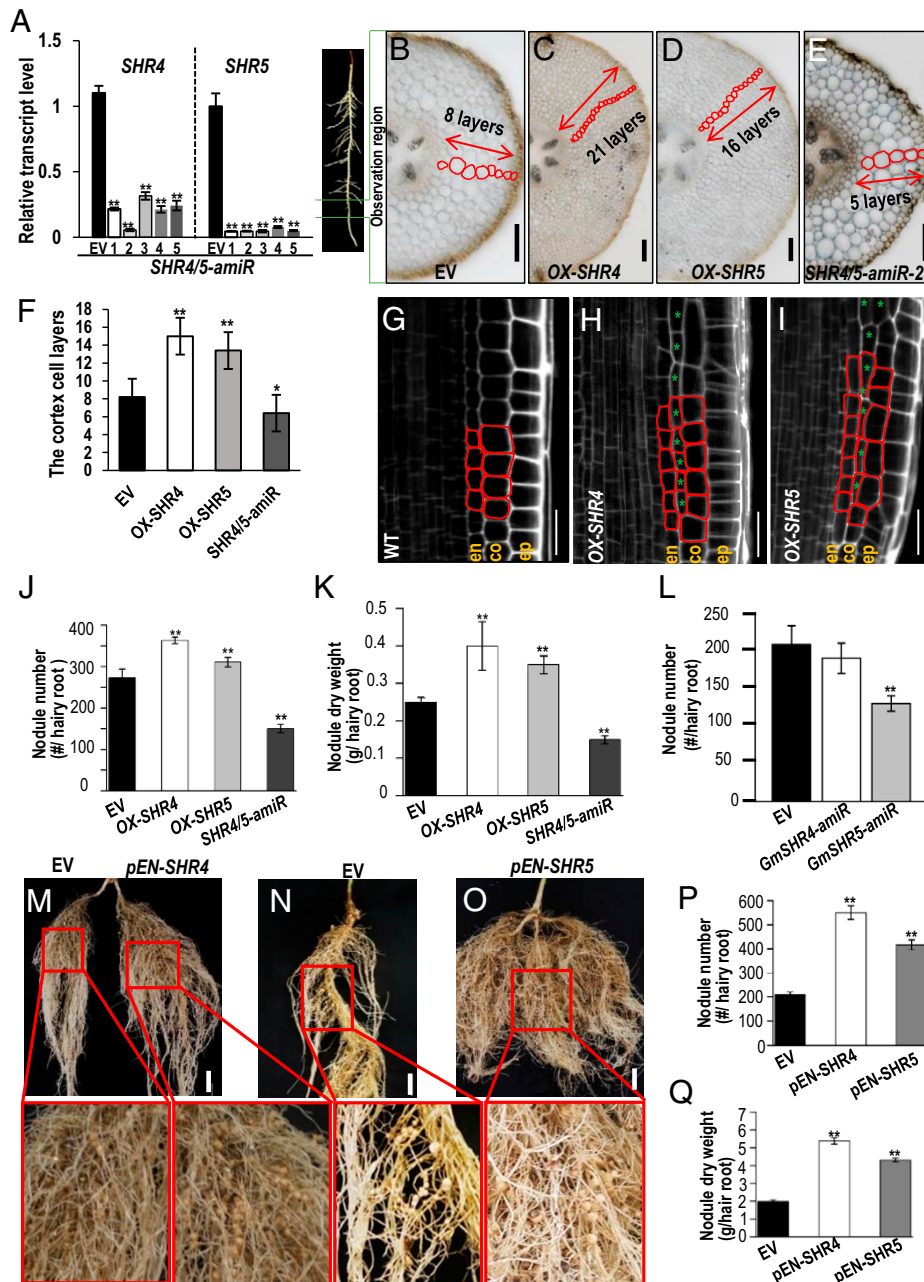


Fig. 2. *GmSHR4/5* expression level affects cortical cell division and root nodulation. (A) qRT-PCR shows that the expression of *GmSHR4* and *GmSHR5* is suppressed in the roots of artificial microRNA lines (*GmSHR4/5-amiR*). The RNA was extracted from the noninoculated roots. Error bars represent SD. *GmEF1 α* (accession no. X56856) was used as the internal control. (B–E) The cortex cell layers in the root cross-section of *GmSHR4/5* overexpression lines (*OX-GmSHR4/5*) and *GmSHR4/5-amiR* lines. All cortex sections were sampled from the same position of the hairy roots ($n \geq 15$). (Scale bars, 100 μ m.) (F) Quantification of the cortex cell layers shown in B–E ($n \geq 15$). (G–I) Extra cortex cell division in the propidium iodide-stained *Arabidopsis* roots with ectopic expression of *GmSHR4* and *GmSHR5* ($n \geq 10$). (Scale bars in G–I, 20 μ m.) Green asterisks point to the extra cortex cells. (J and K) Nodule number (J) and nodule dry weight (K) in roots at 28 dai ($n \geq 25$). (L) Nodule number per root at 28 DAI. ($n \geq 25$). (M–Q) Nodulation in different backgrounds. (M) Split root showing the same root transformed with EV (Left) and *pENOD40-GmSHR4* (Right). (N and O) EV and *pENOD40-GmSHR5*. Lower panels are the close-up views of the roots in M–O. (Scale bars, 2 cm.) (P) Nodule number. (Q) Nodule dry weight. EN, *ENOD40* ($n \geq 20$). Significant differences are observed between transgenic plants and EV plants. (** $P < 0.01$, * $P < 0.05$; Student's *t* test). Error bars represent SD. *n* represents the number of independent biological samples. All experiments were repeated three times.

nodule structure. In addition, divisions throughout the cortex contribute to the formation of nodules.

***GmSHR4/5* Promote Nodule Formation by Activating Cytokinin Signaling.** It is known that cytokinin promotes cortical cell divisions during nodulation (15–24). To dissect the relationship between cytokinin and *GmSHRs*, we examined the expression of

cytokinin-related genes in *GmSHR4/5* transgenic systems. It was previously reported that CRE1/HK1 is the major cytokinin receptor involved in the nodulation of *Medicago sativa* and *L. japonicus* (17, 19). In soybean, we identified three *HK1* homologs (named *GmHK1-1*, *GmHK1-2*, and *GmHK1-3*). Our qRT-PCR results showed that *GmSHR4/5* had different activation targets, with *GmSHR4* regulating *GmHK1-1* and *GmSHR5* targeting *GmHK1-3*

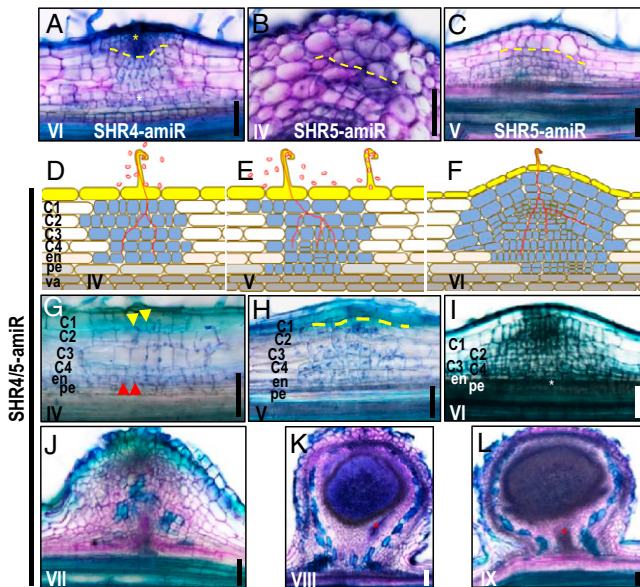


Fig. 3. *GmSHR4/5* function in cortical tissues during the nodulation initiation and affect the formation of nodule vascular tissues. (A) Knockdown of *GmSHR4* did not affect the nodule formation. (B and C) Knockdown of *GmSHR5* leads to the disrupted cortical division in ground tissues. (D–F) Knockdown of both *GmSHR4* and *-5* leads to the disrupted cortical division in ground tissues. (J–L) Knockdown of both *GmSHR4* and *-5* delayed the formation of the vascular tissues in the nodule primordia. Red arrows and white asterisks point to the division of the endodermal cells and pericycle cells, respectively. Yellow dashed lines define the boundary of the division in outer ground tissues or inner ground tissues. Yellow asterisk points to the outer ground tissues. Red asterisks indicate the vascular tissues. Yellow arrows indicate the division of the outer cortical cells ($n \geq 20$). n represents the number of independent biological samples. These experiments were repeated three times with similar results. (Scale bars, 100 μm .)

(Fig. 4A). In support of this, *in situ* hybridization showed that *GmHK1-1* and *GmHK1-3* were expressed in vascular and pericycle cells, as well as in dividing cortical cells (SI Appendix, Fig. S5A and Fig. 4B). In the mature nodule, *GmHK1-3* expression was maintained and mostly restricted to the parenchyma and the infection zone, indicating other regulators might also be involved (Fig. 4B). *In situ* hybridization also showed that *GmHK1-3* expression was noticeably decreased in *GmSHR4/5-amiR* roots (Fig. 4B). Many other genes involved in cytokinin biosynthesis also seemed to be activated by *GmSHR4/5* (Fig. 4A). In *GmSHR4/5-amiR* roots, transcript levels for all these genes were significantly reduced (Fig. 4A). In addition, expression of *CKX3*, a cytokinin oxidase/dehydrogenase gene that negatively regulates cytokinin level, was decreased in *OX-GmSHR4/5* roots and increased in *GmSHR4/5-amiR* roots at 8 dai (Fig. 4A). However, 6-Benzylaminopurine (6-BA) treatment seemed to have little effect on the expression of *GmSHR4/5* (SI Appendix, Fig. S5B). To ensure the accuracy, we further examined the expression of *SHR* and cytokinin-related genes in individual roots of *OX-GmSHR4*, *OX-GmSHR5*, *GmSHR4-amiR*, *GmSHR5-amiR*, and *GmSHR4/5-amiR* (eight roots for each background). The result in Fig. 4A was verified in single-root expression analyses (SI Appendix, Fig. S5D), indicating that *GmSHR4/5* promote nodule formation by activating cytokinin signaling.

To examine how *GmSHR4/5* regulate *GmHK1-3* expression, we performed a yeast one-hybrid (Y1H) assay. We found that *GmSHR4/5* could directly bind to the promoter of *GmHK1-3* (Fig. 4C). To validate this result, we performed chromatin immunoprecipitation (ChIP)-qPCR using transgenic hairy roots expressing *SHR4/5:GFP*. Two primer pairs were designed to target two regions (P1 and P2) in the *GmHK1-3* promoter

(SI Appendix, Table S1). We detected strong enrichment of *GmSHR4/5* in the P1 region of the *GmHK1-3* promoter (Fig. 4D–F).

Finally, we examined the effect of exogenous cytokinin (6-BA) on nodule formation. When the 6-BA concentration was increased from 5 to 10 nM, we started to see an increase in nodule number in the treated groups (SI Appendix, Fig. S6A–D). When *GmSHR4/5-amiR* roots were treated with 10 nM 6-BA, their nodulation phenotype was fully rescued (Fig. 4G and SI Appendix, Fig. S6E–H).

To further examine the function of HK1s, we knocked down their expression (*GmHK1-1,1-2,1-3-amiR* hereafter) in soybean roots (SI Appendix, Fig. S6I). As expected, the total number of nodules was significantly lower on *GmHK1-1,1-2,1-3-amiR* roots (Fig. 4H–J and W).

To examine the genetic interactions between *SHR* and *HK1*, we combined *GmHK1-1,1-2,1-3-amiR* with both *OX-SHR5* and *SHR4/5-amiR* roots in a transgenic hairy root system (SI Appendix, Fig. S6J and K). Compared with *OX-SHR5* roots, *OX-SHR5/GmHK1-1,1-2,1-3-amiR* roots exhibited significantly decreased nodulation, showing the similar phenotypes to *GmHK1-1,1-2,1-3-amiR* roots (Fig. 4H–V). Quantification of nodule numbers confirmed the similarity between *OX-SHR5/GmHK1-1,1-2,1-3-amiR* and *GmHK1-1,1-2,1-3-amiR* roots, suggesting the potential epistasis of HK1 over *SHR5* (Fig. 4X). In addition, no further reduction of nodules was observed in *GmSHR4/5-amiR/GmHK1-1,1-2,1-3-amiR* lines, suggesting they presumably act in the same pathway.

Early Nodulin Genes Act Downstream of *GmSHR4/5*. Cytokinin interacts with Nod factor signaling to control the expression of nodulin genes during nodulation. Therefore, we next examined how *GmSHR4/5* interplay with these symbiotic marker genes (11, 27, 38, 39). We first verified that cytokinin indeed activated the early nodulin genes (SI Appendix, Fig. S4B). Most of the early nodulin genes, including *GmNIN*, *GmNSP1*, and *GmENOD40*, were up-regulated in *OX-GmSHR4/5* roots while down-regulated in *GmSHR4/5-amiR* roots (SI Appendix, Fig. S7A). *In situ* hybridization showed that *GmNIN* was mostly expressed in the pericycle cells (SI Appendix, Fig. S7B), along with weak expression in the epidermis in soybean roots (SI Appendix, Fig. S7B). During nodulation, *GmNIN* was mainly expressed in the dividing cortical cells (SI Appendix, Fig. S7C). Notably, *GmNIN* expression was noticeably decreased in *GmSHR4/5-amiR* roots (SI Appendix, Fig. S7E–G). Conversely, we also tested whether *GmSHR4/5* expression was affected by the early nodulin genes. In the soybean roots overexpressing *GmENOD40* or *GmNSP1*, we detected no dramatic change in the expression of *GmSHR4* (SI Appendix, Fig. S7H). However, *GmSHR5* was surprisingly down-regulated in the presence of high levels of *GmENOD40* or *GmNSP1* (SI Appendix, Fig. S7H). These findings suggest that *GmSHR4/5* likely function upstream of early nodulin genes but that *GmSHR5* expression may be subject to feedback inhibition by these genes, which could partially explain why *GmSHR5* transcript levels were dramatically reduced during the later stages of the nodulation. Furthermore, our Y1H results showed that *GmSHR4* directly targeted the *GmNSP1* promoter for activation (SI Appendix, Fig. S7I). Therefore, we concluded that these early nodulin genes are downstream components of the *GmSHR4/5* and cytokinin signaling pathway.

***GmCYCD6;1* Homologs Are Functional Components of *GmSHR4/5*-Mediated Nodulation.** In *Arabidopsis*, *SHR* regulates periclinal cell divisions by promoting the specific expression of a D-type cyclin, *CYCD6;1* (35). Therefore, we asked whether this conserved module is part of the developmental program for nodulation in soybean. In the *G. max* genome, there are six *GmCYCD6;1* homologs (named *GmCYCD6;1-1* to *GmCYCD6;1-6*). Phylogenetic analysis

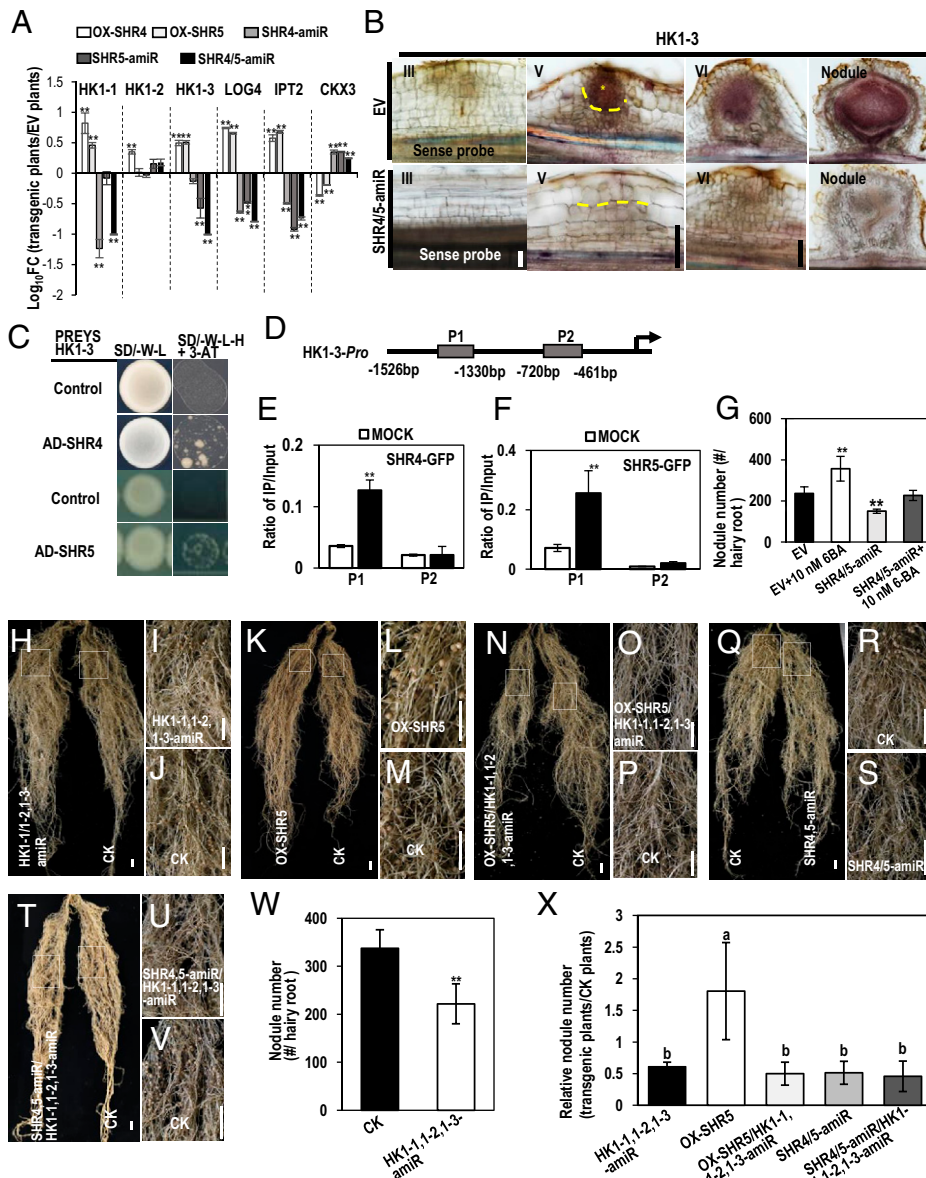


Fig. 4. GmSHR4 and GmSHR5 function upstream of cytokinin signaling during nodulation. (A) The relative transcript of cytokinin genes in EV, *OX-GmSHR4*, *OX-GmSHR5*, *GmSHR4-amiR*, *GmSHR5-amiR*, and *GmSHR4/5-amiR* lines. The RNA was extracted from the noninoculated roots. *GmEF1 α* (accession no. X56856) was used as the internal control. Significant differences are observed between transgenic plants and EV plants. (** $P < 0.01$; Student's *t* test). Error bars represent SD. (B) In situ hybridization of *GmHK1-3* in EV and *GmSHR4/5-amiR* lines. Yellow asterisk marks the division in outer ground tissues. Yellow dashed line defines the division in outer ground tissues ($n \geq 10$). (C) Y1H assays showing the interaction between GmSHR4/5 and *HK1-3* promoter. Promoters in pHIS 2 vector and pGADT7-GmSHR4/5 were cotransformed into yeast strain Y187. The empty pGADT7 vector (AD) was used as the negative control. The yeast clones were grown on SD/-Leu/-His/-Trp (-L-W-H) medium with 60 mM 3-AT ($n = 3$). (D) Regions of the *GmCYCD6;1-6* promoter were used for ChIP (P1 to P2) assays. (E and F) The ratio of bound promoter fragments versus total input detected by qRT-PCR after immunoprecipitation of GFP-GmSHR4/5 by GFP antibodies. Data are means (\pm SE), $n = 3$. (G) The exogenous 6-BA can rescue the defective nodulation in *GmSHR4/5-amiR* roots. Shown is nodule number in roots with 10 nM 6-BA treatment ($n \geq 20$). (H–V) Nodulation in *GmHK1-1,1-2,1-3-amiR*, *OX-GmSHR5/GmHK1-1,1-2,1-3-amiR* roots and *GmSHR4/5-amiR/GmHK1-1,1-2,1-3-amiR* roots. (I and J) Close-up view of the boxed areas in H. (L and M) Close-up view of the boxed areas in K. (O and P) Close-up view of the boxed areas in N. (R and S) Close-up view of the boxed areas in Q. (U and V) Close-up view of the boxed areas in T. (W and X) Nodule number. The roots were examined at 16 dai with rhizobia. Significant differences are observed between transgenic plants and CK plants (** $P < 0.01$, * $P < 0.05$; Student's *t* test). Error bars represent SD. Different letters indicate significant differences between genotypes ($P < 0.05$ by Tukey's test). (Scale bars, 1 cm.) CK, control check.

revealed that *GmCYCD6;1-1* to *GmCYCD6;1-4* are closely related to *Arabidopsis AtCYCD6;1* but *GmCYCD6;1-5* and *GmCYCD6;1-6* are distally related (SI Appendix, Fig. S8A). Transcriptional analysis showed that all *GmCYCD6;1s* were substantially up-regulated in *OX-GmSHR4/5* roots and significantly down-regulated in *GmSHR4/5-amiR* roots (SI Appendix, Fig. S8B). We further examined the spatial expression patterns of *GmCYCD6;1* using in situ hybridization. The results showed that

GmCYCD6;1-1, *GmCYCD6;1-2*, *GmCYCD6;1-3*, *GmCYCD6;1-4*, and *GmCYCD6;1-5* were all expressed in the vascular tissues (SI Appendix, Fig. S8 C–Q). In contrast, both in situ hybridization and the promoter:GUS reporter showed that *GmCYCD6;1-6* expression was mostly enriched in the dividing cortical cells (SI Appendix, Fig. S8 S, U, and V). In mature nodules, *GmCYCD6;1-6* was expressed in nodule parenchyma (SI Appendix, Fig. S8W).

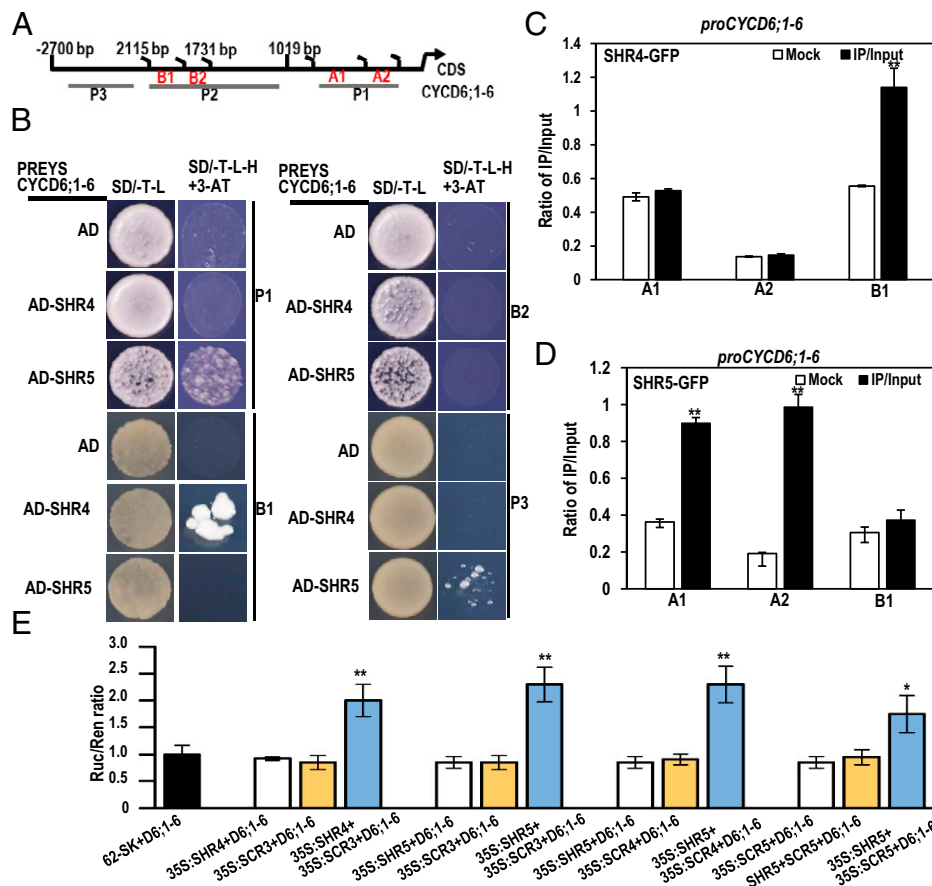


Fig. 5. D-type cyclins act downstream of *GmSHR4/5* to promote nodulation. (A) Regions of the *GmCYCD6;1-6* promoter were used for ChIP and Y1H assays (A–D). (B) Y1H analyses of the interaction between *GmSHR4/5* and the promoter of *CYCD6;1-6* ($n = 3$). (C and D) The ratio of bound promoter fragments versus total input detected by qRT-PCR after immunoprecipitation of GFP-*GmSHR4/5* by GFP antibodies. Data are means (\pm SE), $n = 3$. (E) LUC activation reporter assays. D6 represents the reporter of *CYCD6;1-6* promoter. D6, *CYCD6* ($n = 3$). Asterisks indicate significant differences using Student's *t* test (* $P < 0.05$; ** $P < 0.01$).

Next, we performed a Y1H assay to determine whether the regulation of *GmCYCD6;1-6* by *GmSHR4/5* is direct. We tested four regions of the *GmCYCD6;1-6* promoter (P1, B1, B2, and P3), as shown in Fig. 5A. We found that *GmSHR4* and *GmSHR5* directly bound to the B1 and P1 regions of the *GmCYCD6;1-6* promoter (Fig. 5B). To validate this result, we performed ChIP-qPCR using transgenic hairy roots expressing *35S:GmSHR4/5-GFP*. To detect immunoprecipitated DNA fragments bound by *GmSHR4/5-GFP*, we designed primers targeting the *GmCYCD6;1-6* promoter (regions A1, A2, and B1) (Fig. 5A). We observed a 2.05-fold enrichment of *GmSHR4* in region B1 (Fig. 5C) and 2.48- and 5.15-fold enrichments of *GmSHR5* in regions A1 and A2, respectively (Fig. 5D). Despite these results, we failed to detect the activation of *GmCYCD6;1-6* by *GmSHR4/5* in the LUC activation reporter system (Fig. 5E).

In *Arabidopsis*, *AtSHR* was reported to form a complex with *AtSCR* to activate *CYCD6;1* (35). To see whether this mechanism is also conserved in soybean, we next examined the effect of *GmSCRs* on the expression of *GmCYCD6;1-6*. There are six *GmSCR* genes in the soybean genome, clustering into four groups in our phylogenetic analysis (SI Appendix, Fig. S9A). Using Y2H assays, we detected physical interactions between multiple *GmSHR-GmSCR* pairs (*GmSHR4* and *GmSCR3*, *GmSHR5* and *GmSCR3*, and *GmSCR4* and *GmSCR5*) (SI Appendix, Fig. S9B). We then tested whether the various *GmSCRs* can help activate *GmCYCD6;1-6*. In a LUC reporter system, we indeed detected activation of *GmCYCD6;1-6* when both *GmSHR* and *GmSCR* were added (Fig. 5E).

***GmCYCD6;1s* Function Downstream of Early Nodulin Genes.** In *OX-GmENOD40*, *OX-GmNSP1*, and *OX-GmNSP2* roots, the expression of *GmCYCD6;1-3* to *GmCYCD6;1-6* was markedly increased, while the expression of *GmCYCD6;1-1* and *GmCYCD6;1-2* seemed to be increased only in *OX-GmENOD40* and *OX-GmNSP2* roots (Fig. 6A). Although the transcriptional analysis supported that *GmCYCD6;1s* function downstream of early nodulin genes, *GmCYCD6;1* seemed to have a feedback effect on nodulin gene expression. When *GmCYCD6;1-2* was overexpressed in soybean roots (Fig. 6B), the expression of *GmNSP1* and *GmNSP2* was up-regulated (Fig. 6B). Interestingly, the spatial expression pattern of *pGmENOD40:GUS* was similar to that of *pGmCYCD6;1-6:GUS* (SI Appendix, Figs. S8R–W and S9C–F).

Cytokinin is a key regulator of root nodulation and the nodulin genes (23, 26). In soybean roots, cytokinin also markedly activated the expression of *GmCYCD6;1-3/4/6* (SI Appendix, Fig. S5C). We next examined the role of the *GmCYCD6;1* genes in soybean root nodulation. We manipulated the expression of three of the *GmCYCD6;1* genes by overexpression and microRNA-mediated knockdown (SI Appendix, Fig. S10A and B). As shown in SI Appendix, Figs. S7C–R and S9C–J, overexpression of *GmCYCD6;1-2*, *GmCYCD6;1-3*, and *GmCYCD6;1-6* all significantly increased nodulation, as evidenced by increased nodule number, total nodule fresh weight, and nodule size. By contrast, knockdown of any of these three *GmCYCD6;1* genes resulted in inhibition of nodulation. These results indicate that the *GmCYCD6;1* genes function as positive regulators of soybean nodulation downstream of the early nodulation genes.

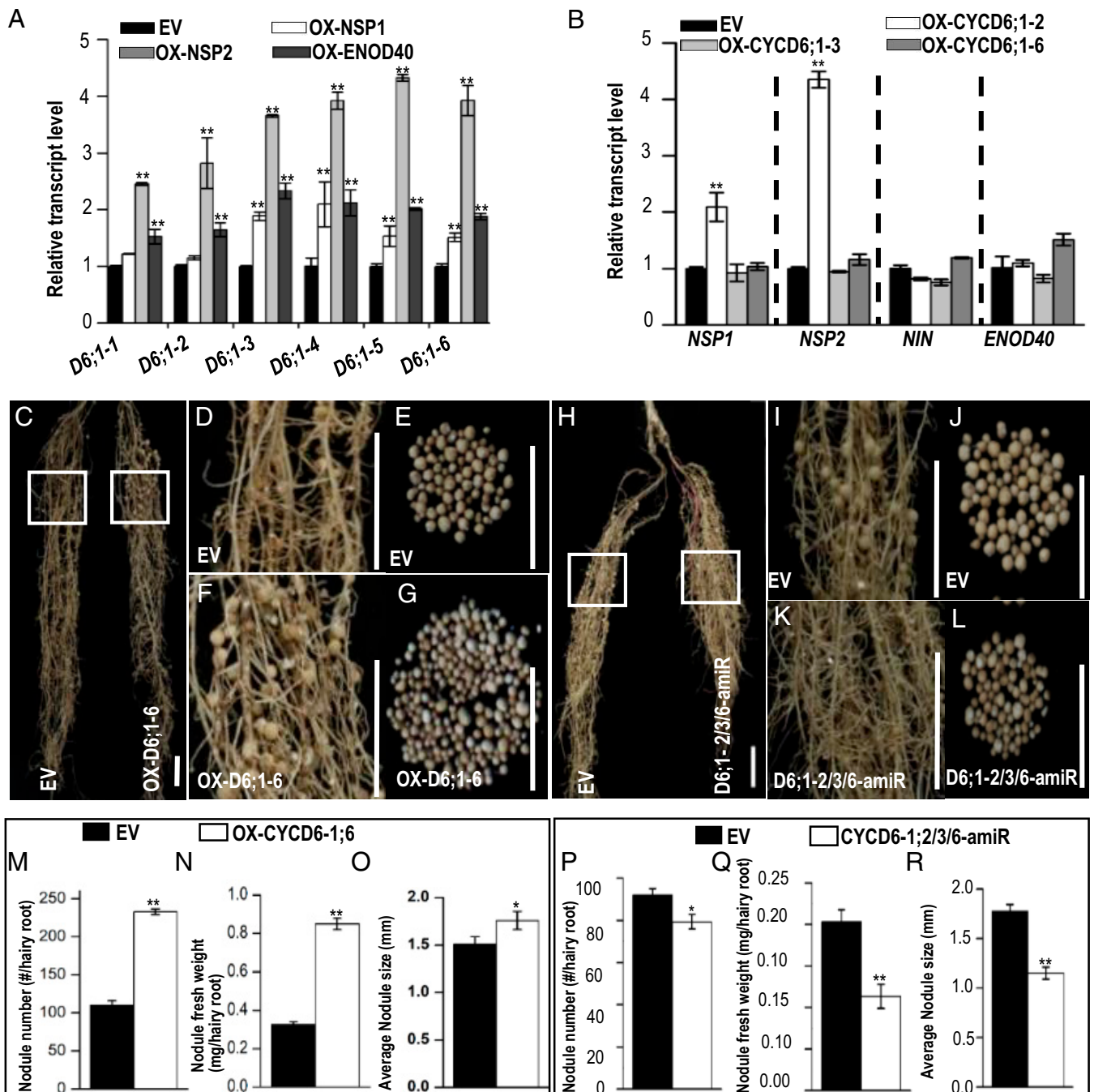


Fig. 6. D-type cyclins act downstream of early nodulin genes. (A) The relative expression of *GmCYCD6;1s* in EV and the *OX-GmNSP1*, *OX-GmNSP2*, and *OX-GmENOD40* lines. The RNA was extracted from the noninoculated roots. *GmEF1 α* (accession no. X56856) was used as the internal control. Significant differences are observed between transgenic plants and EV plants (** $P < 0.01$, * $P < 0.05$; Student's t test). Error bars represent SD. D6, *CYCD6* ($n = 3$). (B) The relative expression of early nodulin genes in EV and the *OX-GmCYCD6;1-2*, *OX-GmCYCD6;1-3*, and *OX-GmCYCD6;1-6* lines. *GmEF1 α* (accession no. X56856) was used as the internal control. Significant differences are observed between transgenic plants and EV plants (** $P < 0.01$, * $P < 0.05$; Student's t test). Error bars represent SD ($n = 3$). (C–G) Nodulation in *OX-GmCYCD6;1-6* roots. D6, *GmCYCD6*. (D and F) Close-up view of the boxed areas in C. (Scale bars: C, 2 cm; D and F, 5 mm.) (H–L) Nodulation in *CYCD6;1-2/3/6-amiR* roots. (I and K) Close-up view of the boxed areas in H. (Scale bars: H, 2 cm; I and K, 5 mm.) (M–R) The quantification of the nodulation in *OX-CYCD6;1-6* roots and *CYCD6;1-2/3/6-amiR*. Shown are nodule number (M and P), nodule fresh weight (N and Q), and nodule size (O and R) ($n \geq 18$). Significant differences are observed between transgenic plants and EV plants (** $P < 0.01$, * $P < 0.05$; Student's t test). Error bars represent SD. n represents the number of independent biological samples. All experiments were repeated three times.

Spatially Separated Cortical Cell Divisions Account for the Formation of Nodule Primordia and Vascular Founder Cells. The two distinct locations of cortical cell divisions in the early stage of nodulation prompted us to hypothesize that the cell divisions in the

outer cortical layers are mainly responsible for the formation of nodule primordia and the divisions in the inner cortex produce the founder cells for the vascular tissues of the nodules. To test this hypothesis, we first examined the expression of *GmSHR1*

in nodule, a close homolog of *AtSHR*, which is expressed when the vascular founder cells are initiated in the globular stage of embryo development (39). Similar to *AtSHR*, *GmSHR1* had a specific expression in the stele (SI Appendix, Figs. S2E and S11A). The *GmSHR1* was not induced by the rhizobia inoculation, but showed patchy expression underlying the newly formed nodule primordia (SI Appendix, Fig. S11B–D). This expression persisted and gradually became restricted to the newly formed vascular tissues of the nodule (SI Appendix, Fig. S11E and F). In line with this hypothesis, knockdown of *GmSHR4/5* considerably disrupted the cell divisions in inner cortex and affected the formation of nodule vascular tissues (Fig. 3J–L).

In the outer cortex, repeated cell divisions drove the emergence of primordia-like structures from the soybean roots (SI Appendix, Fig. S3E, K, and P). This bulging tissue was similar in morphology to the lateral root primordia. We therefore tested whether the primordia-like structures have stem cells by examining the expression of the marker gene *GmWOX5*. In situ hybridization showed that expression of *GmWOX5* was initiated in the early stage of nodulation, when the bulging structures were formed (SI Appendix, Fig. S11G). The spatial expression of *GmWOX5* in these structures was very similar to that in lateral roots, with enrichment in a few cells located at the top of the bulging tissue (SI Appendix, Fig. S11H). In the mature nodule, *GmWOX5* expression was maintained, but was mostly restricted to the nodule parenchyma (SI Appendix, Fig. S11I).

Discussion

Several lines of evidence have shown that nodule organogenesis is evolutionarily related to root development (5, 28, 29). Genes important for regulating root stem cells, including *WOX5* and *PLETHORA* (*PLT1-4*), play vital roles in the establishment of root nodule primordia (32–34). Nodule-specific knockdown of *MtPLETHORA* genes results in a reduced number of nodules or generates nodules with inactive meristems. Similar to lateral root development, nodule organogenesis starts from oriented cell divisions in root cortical tissues. However, we still have very limited understanding of the mechanism behind this cortical cell division during nodulation. In *Arabidopsis* roots, *SHR-SCR-CYCD6;1* forms a regulatory module that spatiotemporally promotes periclinal cell divisions in cortex/endodermis initials (35). There is also evidence that *AtSHR* and rice *SHR* homologs can induce periclinal cell divisions in cortical tissues in root meristem (40, 41). The first cell division of a determinate nodule (such as those of soybean) occurs subepidermally in the outer cortex (42, 43). In this study, we provide evidence demonstrating that two *SHR* paralogs in soybean regulate nodulation by promoting cortical cell divisions in the cortex.

We identified six *SHR* homologs in soybean, which were differentially expressed in roots, stems, leaves, and nodules, implying that *GmSHR* could participate in a wide range of developmental processes in soybean. Four of the soybean *SHR* homologs are closely related to *AtSHR* and *MtSHR1* (*Medtr5g015490*) (36) and exhibited a similar vascular expression pattern, while two distal paralogs (*GmSHR4* and *GmSHR5*) had a distinct expression pattern. This implies that subfunctionalization of *SHR* homologs may have occurred during soybean evolution. Interestingly, *GmSHR4* and *GmSHR5* exhibited high levels of expression in the initial stage of nodule development, when nodule vascular tissues had not yet formed. In contrast, *GmSHR1* and *GmSHR2* were also induced during nodulation but were specifically expressed in the vascular tissues of the mature nodules. These results suggest that *GmSHR* family members may differentially regulate different stages of soybean nodulation. Upon the *Rhizobial* infection, the expression of *GmSHR4/5* was activated in outer cortical cells, where nodule primordia were initiated. In the outer cortical cells, *GmSHR5* seemed to play a more dominant role as the

inhibition of *GmSHR5* affected the formation of the nodule primordia. However, *GmSHR4* and *GmSHR5* could also be functionally redundant during nodulation. The overexpression of either of these two *GmSHR* genes substantially improved nodulation, suggesting that they could functionally replace each other.

Previous studies revealed that cytokinin signaling interacts with Nod factors to promote cortical cell division during nodulation (24). Although we know that a number of early nodulin genes are involved, the detailed mechanism of this stimulation of cortical cell division remains a mystery and it is not clear how the upstream signaling cascade is transduced to regulate cell division. Our results provide evidence that soybean *GmSHR4/5* are a signaling component downstream of Nod factor perception but upstream of cytokinin as well as early nodulin genes, including *GmNSP1*, *GmNIN*, and *GmENOD40*. Interestingly, this regulation seems to involve a complex network rather than a linear cascade. A recent report showed increased *MtSHR1* expression after 6-BA treatment in *Medicago*, and 6-BA effect seemed to be abolished in *MtSHR1-SRDX* hairy roots (36). However, in soybean roots, 6-BA treatment was insufficient to promote *GmSHR4/5* expression and genetic analysis showed that *GmHK1* presumably functions downstream of *GmSHR4/5* during the nodulation in soybean. This difference might reflect the differential mechanism between indeterminate nodules and determinate nodules.

The expression of *GmSHR5* could be suppressed when *GmNSP1* and *GmENOD40* were overexpressed. This potential feedback loop is also evidenced by the differential ability of *GmSHR4* and *GmSHR5* to induce nodules. Compared to the substantially increased nodule number induced by overexpression of *GmSHR4*, overexpression of *GmSHR5* only moderately enhanced nodulation, which may reflect the feedback inhibition of *GmNSP1* on *GmSHR5*. Both *GmSHR4* and *GmSHR5* seemed to play roles only in the early stage of nodulation, as their expression was hard to detect in mature nodules. Therefore, *GmSHR4/5* could represent a key regulatory module of NFR-mediated early symbiotic events.

ENOD40 was previously shown to promote cortical cell division (44). However, the link between *ENOD40* and downstream mitosis is not known. Here we showed that *GmENOD40* induced the expression of D-type cyclins. Considering the role of the *Arabidopsis* D-type cyclin homolog (*AtCYCD6;1*) in promoting periclinal cell division, it is likely *GmENOD40* promotes cortical cell division during nodulation by inducing *GmCYCD6;1* expression. In line with this, *GmCYCD6;1* expression in soybean roots was also enhanced by the application of cytokinin, which could induce spontaneous nodules without rhizobial infection.

In *Arabidopsis*, it was discovered that *AtSHR* regulates the development of vascular tissues by repressing cytokinin biosynthesis (45). Interestingly, in poplar, *PtSHR1* seemed to increase cytokinin biosynthesis to promote both primary (height) and secondary (girth) growth (46). Soybean has six *SHR* homologs that can be clustered into two groups. *GmSHR4/5* not only are distally related to the other *GmSHR* genes phylogenetically, but also exhibited expression patterns distinct from the other *GmSHR* genes. This suggests that the *GmSHR* genes have likely undergone subfunctionalization during their evolution. Through multiple assays, we showed that soybean *SHRs* promote nodulation by enhancing both cytokinin biosynthesis and signaling. In addition, *GmSHR4/5* seemed to promote *GmCYCD6;1-6* expression by directly binding to its promoter. This direct activation mechanism appears to be evolutionarily conserved as a similar mechanism also exists in *Arabidopsis* roots. Finally, *GmSHR4/5* can also activate the expression of D-type cyclins via the early nodulins *GmNIN* and *GmENOD40*. The two *SHR*-mediated cascades that activate D-type cyclins form a classic feedforward loop to ensure the progression of nodule organogenesis (SI Appendix, Fig. S12).

Materials and Methods

Additional materials and methods are described at length in *SI Appendix, SI Materials and Methods*.

G. max cv. Williams-82 seeds and rhizobium strain *Bradyrhizobium* sp. BXVD3 were used throughout the experiments. Roots or nodules for histological analysis were embedded in a 5% agarose gel and 100- μ m sections were obtained with a microtome (Leica VT1000S). Details are provided in *SI Appendix, SI Materials and Methods*.

Accession numbers are listed in *SI Appendix, Table S2*.

Data Availability.

qRT-PCR, GUS staining, construction of phylogenetic tree, genetics assay, in situ, and biochemistry assay data (Glyma.01G194200, Glyma.05G105600, Glyma.11G047700, Glyma.13G345700, Glyma.15G028600, Glyma.17G160800, Glyma.13G303000, Glyma.12G199300, Glyma.12G105600, Glyma.06G299700, Glyma.13G247600, Glyma.15G066200, Glyma.07G039400, Glyma.04G251900,

Glyma.11G188100, Glyma.03G181300, Glyma.07G158800, Glyma.08G049000, Glyma.07G173700, Glyma.17G054500, Glyma.04G000600, Medtr8g020840.1, Glyma.01G028500, Glyma.03G123800, Glyma.02g42200, Glyma.09G270000, Glyma.11G096500, Glyma.12G022600, Glyma.10G038500) have been deposited in Phytozome. Construction of phylogenetic tree data (Solyc02g092370) have been deposited in Sol Genomics Network. Construction of phylogenetic tree data (AT4G37650 and AT4G03270) have been deposited in Tair. Construction of phylogenetic tree data (AJ832138, ABK35066.1, ABG49438.1, AAP06856.1, NP_192565.1, AJ832139, XP_012574062.1, XP_020232189.1) have been deposited in NCBI. All other study data are included in this article and/or *SI Appendix*.

ACKNOWLEDGMENTS. We thank Dr. Hong Liao for sharing research materials. This work is supported by the National Key Research and Development Program of China (2016YFD0100700, 2018YFD1000800) and the National Natural Science Foundation of China (31722006).

1. H. Nishida, T. Suzuki, Nitrate-mediated control of root nodule symbiosis. *Curr. Opin. Plant Biol.* **44**, 129–136 (2018).
2. D. Tsikou *et al.*, Systemic control of legume susceptibility to rhizobial infection by a mobile microRNA. *Science* **362**, 233–236 (2018).
3. M. Crespi, F. Frugier, De novo organ formation from differentiated cells: Root nodule organogenesis. *Sci. Signal.* **1**, re11 (2008).
4. B. J. Ferguson *et al.*, Molecular analysis of legume nodule development and autoregulation. *J. Integr. Plant Biol.* **52**, 61–76 (2010).
5. G. J. Desbrosses, J. Stougaard, Root nodulation: A paradigm for how plant-microbe symbiosis influences host developmental pathways. *Cell Host Microbe* **10**, 348–358 (2011).
6. G. E. Oldroyd, Speak, friend, and enter: Signalling systems that promote beneficial symbiotic associations in plants. *Nat. Rev. Microbiol.* **11**, 252–263 (2013).
7. H. E. Calvert, M. K. Pence, M. Pierce, N. S. Malik, W. D. Bauer, Anatomical analysis of the development and distribution of Rhizobium infections in soybean roots. *Botany* **62**, 2375–2384 (1984).
8. L. Schauser, A. Roussis, J. Stiller, J. Stougaard, A plant regulator controlling development of symbiotic root nodules. *Nature* **402**, 191–195 (1999).
9. T. Soyano, H. Kouchi, A. Hirota, M. Hayashi, Nodule inception directly targets NF-Y subunit genes to regulate essential processes of root nodule development in *Lotus japonicus*. *PLoS Genet.* **9**, e1003352 (2013).
10. W. C. Yang *et al.*, Characterization of GmENOD40, a gene showing novel patterns of cell-specific expression during soybean nodule development. *Plant J.* **3**, 573–585 (1993).
11. M. D. Crespi *et al.*, enod40, a gene expressed during nodule organogenesis, codes for a non-translatable RNA involved in plant growth. *EMBO J.* **13**, 5099–5112 (1994).
12. B. Compain, W. C. Yang, T. Bisseling, H. Franssen, ENOD40 expression in the pericycle precedes cortical cell division in Rhizobium-legume interaction and the highly conserved internal region of the gene does not encode a peptide. *Plant Soil* **230**, 1–8 (2001).
13. S. Hirsch *et al.*, GRAS proteins form a DNA binding complex to induce gene expression during nodulation signaling in *Medicago truncatula*. *Plant Cell* **21**, 545–557 (2009).
14. S. Hayashi *et al.*, Transient Nod factor-dependent gene expression in the nodulation-competent zone of soybean (*Glycine max* [L.] Merr.) roots. *Plant Biotechnol. J.* **10**, 995–1010 (2012).
15. M. Miri, P. Janakirama, M. Held, L. Ross, K. Szczyglowski, Into the root: How cytokinin controls rhizobial infection. *Trends Plant Sci.* **21**, 178–186 (2016).
16. H. Liu, C. Zhang, J. Yang, N. Yu, E. Wang, Hormone modulation of legume-rhizobial symbiosis. *J. Integr. Plant Biol.* **60**, 632–648 (2018).
17. J. Plet *et al.*, MtCRE1-dependent cytokinin signaling integrates bacterial and plant cues to coordinate symbiotic nodule organogenesis in *Medicago truncatula*. *Plant J.* **65**, 622–633 (2011).
18. A. B. Heckmann *et al.*, Cytokinin induction of root nodule primordia in *Lotus japonicus* is regulated by a mechanism operating in the root cortex. *Mol. Plant Microbe Interact.* **24**, 1385–1395 (2011).
19. M. Held *et al.*, *Lotus japonicus* cytokinin receptors work partially redundantly to mediate nodule formation. *Plant Cell* **26**, 678–694 (2014).
20. B. J. Ferguson, U. Mathesius, Phytohormone regulation of legume-rhizobia interactions. *J. Chem. Ecol.* **40**, 770–790 (2014).
21. F. Frugier, S. Kosuta, J. D. Murray, M. Crespi, K. Szczyglowski, Cytokinin: Secret agent of symbiosis. *Trends Plant Sci.* **13**, 115–120 (2008).
22. S. Boivin *et al.*, Different cytokinin histidine kinase receptors regulate nodule initiation as well as later nodule developmental stages in *Medicago truncatula*. *Plant Cell Environ.* **39**, 2198–2209 (2016).
23. P. Gamas, M. Brault, M. F. Jardinaud, F. Frugier, Cytokinins in symbiotic nodulation: When, where, what for? *Trends Plant Sci.* **22**, 792–802 (2017).
24. L. Tirichine *et al.*, A gain-of-function mutation in a cytokinin receptor triggers spontaneous root nodule organogenesis. *Science* **315**, 104–107 (2007).
25. V. Mortier *et al.*, Role of LONELY GUY genes in indeterminate nodulation on *Medicago truncatula*. *New Phytol.* **202**, 582–593 (2014).
26. D. P. Lohar *et al.*, Cytokinins play opposite roles in lateral root formation, and nematode and Rhizobial symbioses. *Plant J.* **38**, 203–214 (2004).
27. T. Vernié *et al.*, The NIN transcription factor coordinates diverse nodulation programs in different tissues of the *Medicago truncatula* root. *Plant Cell* **27**, 3410–3424 (2015).
28. F. Rouffier *et al.*, The *Medicago* species A2-type cyclin is auxin regulated and involved in meristem formation but dispensable for endoreduplication-associated developmental programs. *Plant Physiol.* **131**, 1091–1103 (2003).
29. P. S. Nutman, Physiological studies on nodule formation: I. The relation between nodulation and lateral root formation in red clover. *Ann. Bot. (Lond.)* **12**, 1–96 (1948).
30. T. Soyano, Y. Shimoda, M. Kawaguchi, M. Hayashi, A shared gene drives lateral root development and root nodule symbiosis pathways in *Lotus*. *Science* **366**, 1021–1023 (2019).
31. K. Schiessl *et al.*, NODULE INCEPTION recruits the lateral root developmental program for symbiotic nodule organogenesis in *Medicago truncatula*. *Curr. Biol.* **29**, 3657–3668.e5 (2019).
32. H. J. Franssen *et al.*, Root developmental programs shape the *Medicago truncatula* nodule meristem. *Development* **142**, 2941–2950 (2015).
33. M. A. Osipova *et al.*, Wuschel-related homeobox5 gene expression and interaction of CLE peptides with components of the systemic control add two pieces to the puzzle of autoregulation of nodulation. *Plant Physiol.* **158**, 1329–1341 (2012).
34. B. Roux *et al.*, An integrated analysis of plant and bacterial gene expression in symbiotic root nodules using laser-capture microdissection coupled to RNA sequencing. *Plant J.* **77**, 817–837 (2014).
35. R. Sozzani *et al.*, Spatiotemporal regulation of cell-cycle genes by SHORTROOT links patterning and growth. *Nature* **466**, 128–132 (2010).
36. W. Dong *et al.*, An SHR-SCR module specifies legume cortical cell fate to enable nodulation. *Nature* **589**, 586–590 (2021).
37. H. Cui, P. N. Benfey, Cortex proliferation: Simple phenotype, complex regulatory mechanisms. *Plant Signal. Behav.* **4**, 551–553 (2009).
38. P. Kaló *et al.*, Nodulation signaling in legumes requires NSP2, a member of the GRAS family of transcriptional regulators. *Science* **308**, 1786–1789 (2005).
39. P. Smit *et al.*, NSP1 of the GRAS protein family is essential for rhizobial Nod factor-induced transcription. *Science* **308**, 1789–1791 (2005).
40. S. Wu *et al.*, A plausible mechanism, based upon Short-Root movement, for regulating the number of cortex cell layers in roots. *Proc. Natl. Acad. Sci. U.S.A.* **111**, 16184–16189 (2014).
41. Q. Yu *et al.*, Cell-fate specification in *Arabidopsis* roots requires coordinative action of lineage instruction and positional reprogramming. *Plant Physiol.* **175**, 816–827 (2017).
42. K. Szczyglowski *et al.*, Nodule organogenesis and symbiotic mutants of the model legume *Lotus japonicus*. *Mol. Plant Microbe Interact.* **11**, 684–697 (1998).
43. P. C. van Spronsen, M. Grönlund, C. Pacios Bras, H. P. Spaink, J. W. Kijne, Cell biological changes of outer cortical root cells in early determinate nodulation. *Mol. Plant Microbe Interact.* **14**, 839–847 (2001).
44. C. Charon, C. Johansson, E. Kondorosi, A. Kondorosi, M. Crespi, enod40 induces dedifferentiation and division of root cortical cells in legumes. *Proc. Natl. Acad. Sci. U.S.A.* **94**, 8901–8906 (1997).
45. H. Cui *et al.*, Genome-wide direct target analysis reveals a role for SHORT-ROOT in root vascular patterning through cytokinin homeostasis. *Plant Physiol.* **157**, 1221–1231 (2011).
46. A. Miguel, A. Milhinhos, O. Novák, B. Jones, C. M. Miguel, The SHORT-ROOT-like gene PSHR2B is involved in Populus phellogen activity. *J. Exp. Bot.* **67**, 1545–1555 (2016).